Shear deformation model for reinforced concrete columns

Halil Sezen[†]

Department of Civil and Environment Engineering and Geodetic Science, The Ohio State University, 470 Hitchcock Hall, 2070 Neil Avenue, Columbus, OH 43210, USA

Abstract. Column shear failures observed during recent earthquakes and experimental data indicate that shear deformations are typically associated with the amount of transverse reinforcement, column aspect ratio, axial load, and a few other parameters. It was shown that in some columns shear displacements can be significantly large, especially after flexural yielding. In this paper, a piecewise linear model is developed to predict an envelope of the cyclic shear response including the shear displacement and corresponding strength predictions at the first shear cracking, peak strength, onset of lateral strength degradation, and loss of axial-load-carrying capacity. Part of the proposed model is developed using the analysis results from the Modified Compression Field Theory (MCFT). The results from the proposed model, which uses simplified equations, are compared with the column test data.

Keywords: shear deformation; reinforced concrete column; seismic response; shear failure; shear strength degradation.

1. Introduction

The total lateral deformation of a reinforced concrete (RC) column subjected to lateral loads is the sum of deformations due to flexure, shear, and slip of the longitudinal bars at column ends (Fig. 1). Flexural deformations vary with the moment along the length of column, while the slip deformations are concentrated at column ends and typically are not included in flexural displacements. These two deformation components can be estimated fairly accurately using available models. Shear deformations are the focus of this study with the objective of modeling an envelope of the cyclic lateral load-shear displacement response of a column. Setzler and Sezen (2007) attempted to combine these three deformation components to predict the total lateral deformation of RC columns.

Shear deformations have traditionally been ignored in design and analysis of RC columns mainly because of three reasons: 1) it is not easy to isolate and measure shear deformations in a real structure or during experimental testing in the laboratory, 2) the shear behavior of cracked reinforced concrete is not fully understood, and there is no consensus on how to model shear behavior of beams and columns. As a result, usually semi-empirical models are used in shear design, and 3) shear deformations are relatively small compared to flexural deformations. The

---

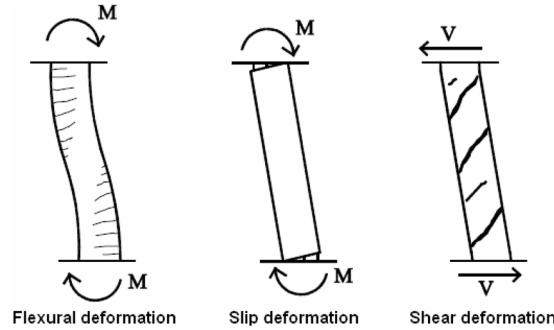† Assistant Professor, E-mail: sezen.1@osu.edu

Fig. 1 Components of lateral deformation in a reinforced concrete column

contribution of shear deformations to total deformations is probably less than 10 percent for a properly designed column (Lehman and Moehle 2000). However, shear deformations can be significant in older existing columns with reinforcement details not meeting the requirements of the current design codes. For example, the test column shown in Fig. 2(a) experienced shear failure after the longitudinal steel yielded and flexural strength was reached. While only about 10 percent of the total lateral displacement, Δ_{total} was due to shear deformations at first flexural yielding, the contribution of shear deformations to total displacement increased to approximately 40 percent at a lateral displacement three times the yield displacement, i.e., at a displacement ductility of 3 (Fig. 3). The experimental data in Fig. 3 indicate that the contribution of shear to the total lateral response increases with increasing displacements as a result of further cracking and damage to member. Four of the five specimens shown in Fig. 3 were tested by Sezen and Moehle (2006), and the last specimen, U6 was tested by Saatcioglu and Ozcebe (1989). These specimens were used later in this paper to validate the proposed shear deformation model.

Modern structural engineering practices aim to prevent shear failure in columns which is brittle and frequently leads to partial or total collapse of the structure. Reinforced concrete buildings constructed prior to 1970s are prone to shear failure, especially in high seismic regions in the
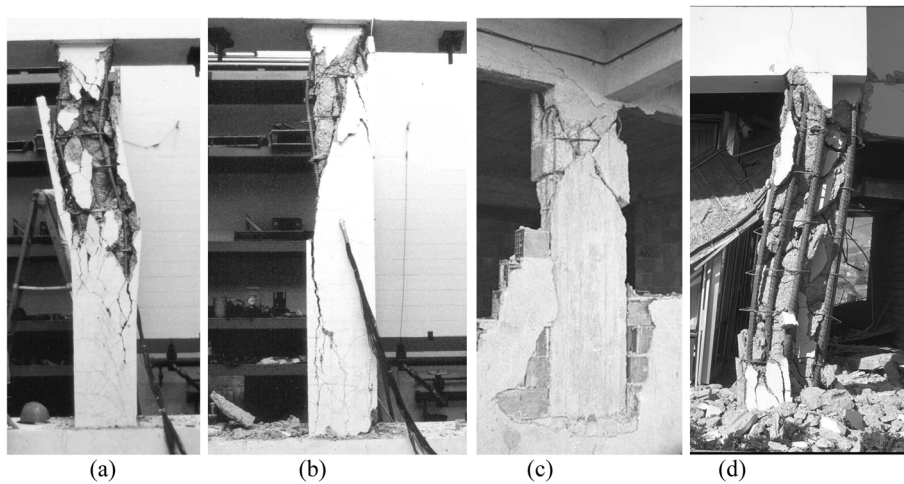

Fig. 2 Shear failure of test columns: (a) Specimen-1, (b) Specimen-2 (Sezen 2002), and column shear failures during: (c) 1999 Kocaeli, Turkey earthquake, and (d) 1971 San Fernando, California earthquake
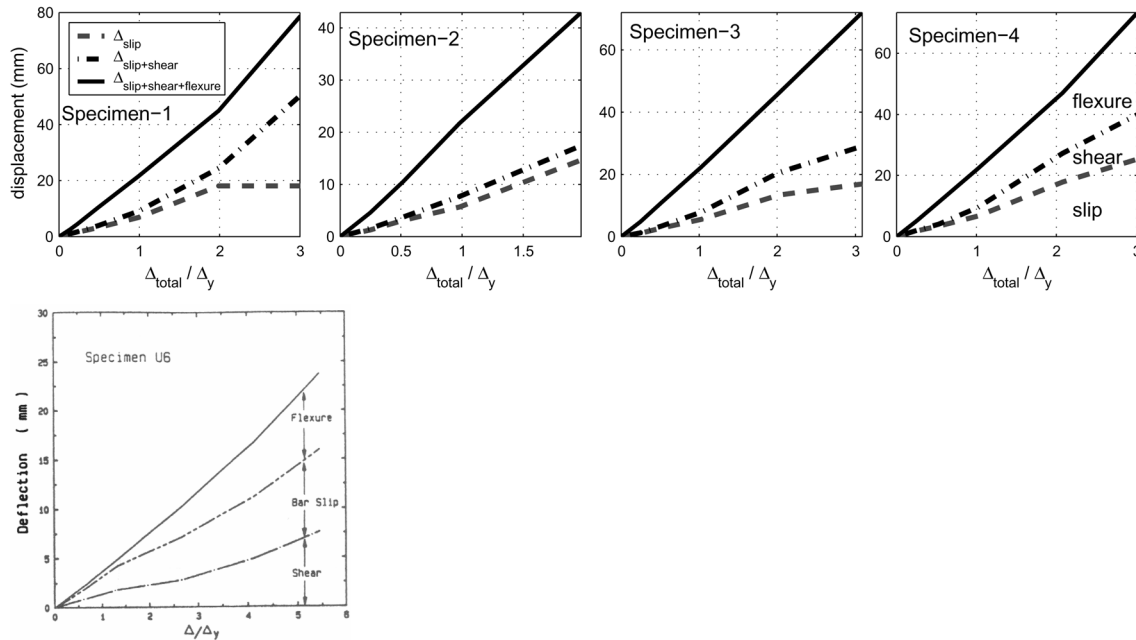
Fig. 3 Contribution of flexure, shear and slip displacements to total displacement

United States, because of insufficient and poor detailing as per the code requirements of that time. Also, in many countries around the world, column shear failure appears to be the most common failure mode leading to structural collapse and loss of life during earthquakes (Fig. 2). Post earthquake reconnaissance (e.g., Aschheim *et al.* 2000, Dogangun 2004) shows that columns with poorly detailed and/or inadequate transverse reinforcement are likely to exhibit large shear deformations, which need to be estimated relatively accurately in order to predict the overall column behavior and to identify potential shear failure. The main objective of this study is to investigate the shear behavior and predict shear deformations of columns experiencing flexural yielding and subsequently failing in shear.

Only few models (e.g., Modified Compression Field Theory, MCFT proposed by Vecchio and Collins (1986 and 1988), softened truss and membrane models by Hsu (1988) and Hsu and Zhu (2002), and the model proposed by Lehman and Moehle 2000) attempted to generate a continuous monotonic lateral load-shear displacement response for RC panels or beam-columns. Many researchers used MCFT analysis results to develop simplified response envelopes. Some of those simplified models will be discussed below. The majority of previous research work related to shear behavior of columns concentrated on prediction of a specific response quantity. For example, ACI Committee 426 (1973) reports an equation to predict the shear strength required to initiate flexure-shear cracks. Shear displacement models at the maximum shear strength are proposed by Park and Paulay (1975) and recently by Gerin and Adebar (2004). Several models are available to predict the maximum shear strength, e.g., ACI 318 (2005), Priestley *et al.* (1994), and Sezen and Moehle (2004). The residual shear strength after shear failure is considered by Pincheira *et al.* (1999).

2. Previous shear models

Most research studies investigating the shear deformations in RC members, including beams, columns and shear walls, are based on the MCFT (Vecchio and Collins 1986 and 1988). Currently the AASHTO bridge design code (American Association of State Highway and Transportation Officials, 2000) uses MCFT for shear design of RC structures. The MCFT is a powerful tool to predict the shear behavior of reinforced concrete including the effect of tensile resistance of cracked concrete. The detailed consideration of tensile resistance of concrete increases both the accuracy and complexity. In addition, in order to satisfy force equilibrium and strain compatibility conditions, an iterative algorithm is required. Currently, MCFT is probably the most accurate available model, however it is complicated to implement. The computer program, Response-2000 (Bentz 2000) which implements MCFT is used in this study to investigate the shear behavior of columns. The program gives the overall lateral load-displacement relations including flexural deformations, however lateral load-shear displacement relations are not readily available in its output. The program calculates the shear strain distribution over the height of the column at each load step. The lateral load-shear displacement relations reported in this paper are determined by integrating these shear strain diagrams over the column height. As shown in Fig. 4, Response-2000 stops its analysis once the peak lateral strength is reached.

It should be noted that the MCFT models the RC shear behavior under monotonically increasing lateral loads only. Similarly, the main objective of this study is to develop a monotonic shear model. Although some researchers (e.g., Maruyama and Jirsa 1979, Takayanagi *et al.* 1979) proposed hysteretic shear models, due to lack of sufficient experimental data and complex nature of the problem, these models were limited in scope. Ozcebe and Saatcioglu (1989) did the pioneering work for hysteretic modeling for shear. In their cyclic model, the monotonic envelope was obtained from the Compression Field Theory (CFT), an older version of MCFT.

Gerin and Adebar (2004) developed a simplified model to predict the lateral load-shear deformation response of membrane elements with uniformly distributed reinforcement in the two directions, e.g., shear walls. As illustrated in Fig. 5(b), the model includes a linear elastic response prior to development of first shear cracks in concrete. The peak lateral strength, V_n is assumed to be
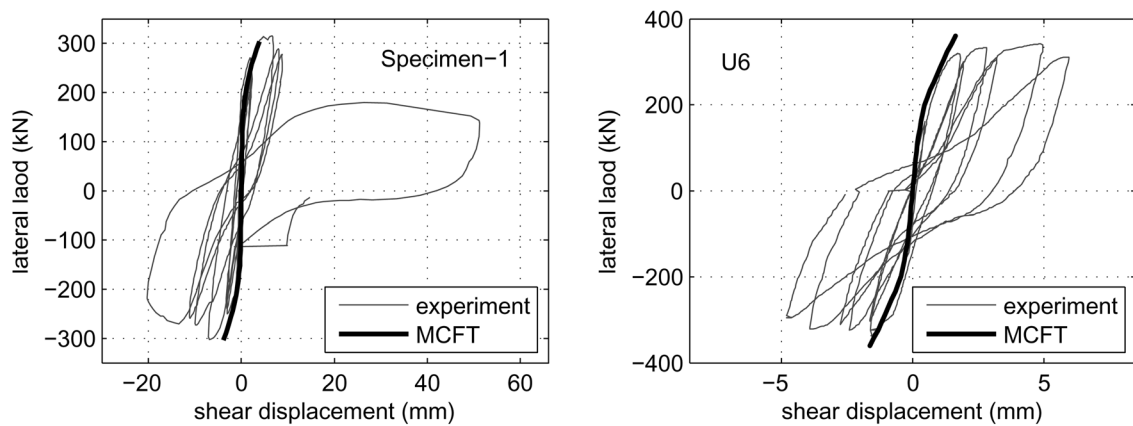

Fig. 4 Comparison of experimental data with MCFT results for Specimen-1 (Sezen 2002) and Column U6 (Saatcioglu and Ozcebe 1989)
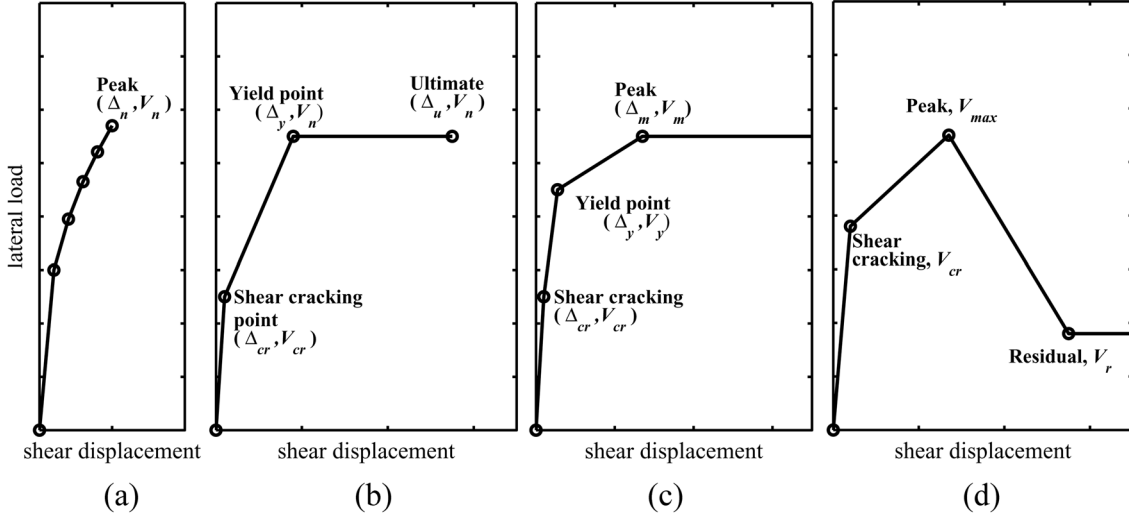
Fig. 5 Lateral load-shear displacement models: (a) MCFT, (b) Gerin and Adebar (2004), (c) Lee and Elnashai (2001), and (d) Pincheira *et al.* (1999)

reached when the horizontal reinforcement yields at a displacement Δ_y. Based on evaluation of test data, a conservative limit for the ultimate shear strain or displacement is also provided.

Ozcebe and Saatcioglu (1989) used the nonlinear MCFT response (Fig. 5(a)) in their models as an envelope or backbone curve as it is, while others such as Lee and Elnashai (2001) and Pincheira *et al.* (1999) represented MCFT response by simplified piecewise linear models (Figs. 5(c) and 5(d)). It should be noted that, in order to be able to create these piecewise linear models or backbone curves, it is necessary first to carry out an MCFT analysis of the RC member using a computer program like Response-2000. In their model, Lee and Elnashai considered both the shear cracking and reinforcement yielding as parameters affecting the shear response. In the model used by Pincheira *et al.*, the effect of shear cracking is recognized and the strength degradation starts immediately after the peak strength is reached. This model was developed primarily to analyze older nonductile columns. Most recently, Mostafaei and Kabeyasawa (2007) proposed a model including the effect of axial-shear-flexure interaction on column behavior. The column shear behavior was incorporated into the model by applying MCFT.

Based on MCFT analysis of column specimens and experimental data, a simplified monotonic shear model is developed in this paper. In the proposed model, the first yielding in the longitudinal steel is not considered as a critical response stage. In other words, the proposed lateral load-shear displacement relationship is independent of the flexural yielding in the column, contrasting most of the available simplified models, including those used by Priestley *et al.* (1996), Gerin and Adebar (2004), and Panagiotakos and Fardis (2001).

3. Proposed model

In order to develop a piecewise linear lateral load-shear displacement relationship or envelope, shear displacements and/or strengths must be predicted at certain critical stages. As shown in Fig. 6, the critical points identified in the proposed model include: first shear cracking (Point A), maximum
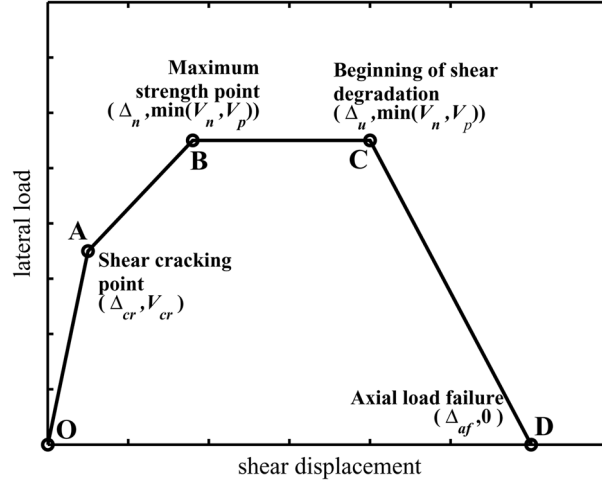
Fig. 6 Proposed monotonic lateral load-shear displacement relationship

shear strength (Point B), onset of strength degradation (Point C), and loss of axial-load-carrying capacity (Point D).

The shear cracking point, identified as Point A in Fig. 6, does not correspond to the first cracking in concrete, which is usually due to flexure. Rather, Point A indicates the initiation of diagonal shear cracks. Either analytically or during the experiments, it is extremely difficult to identify this point clearly, because there will be flexural cracks in the column at this stage and the shear cracks may form as the extension of those pre-existing flexural cracks. MCFT is used here to predict the first shear cracking.

Even though MCFT yields a quite accurate response until the maximum shear strength is reached (Fig. 4), it is based on a relatively complex theory with an iterative algorithm. MCFT does not provide a simple formulation suitable for hand calculations, which would be more useful for practical purposes. In this research, MCFT analysis results were used to develop simple equations to define Points A and B in Fig. 6. To achieve this, it was necessary to first check if MCFT provides certain consistent trends.

For an extensive evaluation of MCFT results, a virtual test matrix consisting of columns with different physical properties, material properties, and load conditions was designed. The columns had properties in the following range: section sizes including 356, 457, and 610 mm square (14, 18, and 24 inches); aspect ratio, a/d (a=shear span, and d=effective section depth) ranging from 2.3 to 9.3; axial load ratio ($P/A_g f_c'$, A_g=gross cross sectional area) varying from 0.05 to 0.62; concrete compressive strength, f_c': 20.7 to 41.4 MPa (3 to 6 ksi); longitudinal steel yield strength, f_{yl}: 276 to 448 MPa (40 to 65 ksi); transverse steel yield strength, f_{yv}: 345 to 483 MPa (50 to 70 ksi); longitudinal steel reinforcement ratio, ρ_l: 1% to 4%; and transverse steel reinforcement ratio, ρ_v: 0.175% to 0.525%.

The above ranges of parameters cover most reinforced concrete columns exhibiting shear, shear-flexure, and flexure failures. To observe the effect of a certain column parameter, only that property was varied while keeping all parameters the same, creating a large matrix. Note that the aspect ratios were also varied in the analyses to extend the evaluations well into the pure shear and pure flexure failure ranges. Specimen-1 (Sezen 2002) was used as the control specimen or "standard
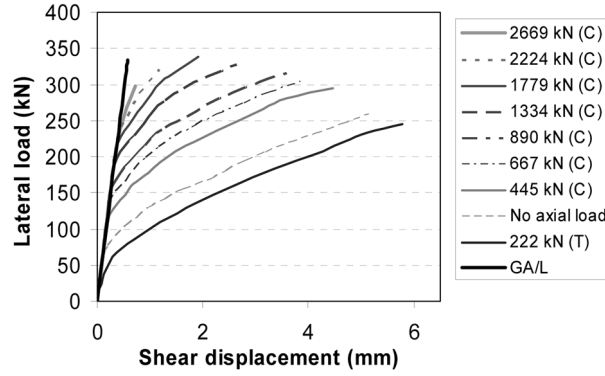
Fig. 7 Shear response of test column, Specimen-1 subjected to different axial loads

column" for developing the test matrix.

Fig. 7 shows the shear response of Specimen-1 under different axial loads. Each curve has the same initial stiffness, evidently independent of the compressive axial load. The unique deviation points in Fig. 7 are observed to correspond to the beginning of shear cracking, which happens much after formation of flexural cracks as per MCFT. In other words, flexural cracking does not seem to affect the shear stiffness. Obviously, flexural cracking greatly influences the flexural stiffness of the column, which is not the subject of this paper. The shear response after shear cracking seems to depend very much on the axial load level as all other parameters are unchanged. The plots in Fig. 7 indicate that the cracked shear stiffness increases with increasing axial load. This is expected because the increase in axial load tends to make the column stiffer, reducing the displacements. However, the initial shear stiffness is somewhat different under tensile or zero axial load. All columns in the test matrix exhibited very similar behavior. Detailed analysis results can be found in Patwardhan (2005). Based on these observations, an initial shear stiffness was defined to represent the response prior to the first shear cracking (slope of line OA in Fig. 6).

3.1 Uncracked shear stiffness

Evaluation of calculated MCFT responses showed that the uncracked shear stiffness can be satisfactorily predicted using the principles of elasticity from Eq. (1), which is based on the assumption that the shear stress distribution is uniform over the cross section of column. This is a reasonable assumption for reinforced concrete members.

$$\Delta_{cr} = \frac{V_{cr}L}{GA_g} \tag{1}$$

where L = column length, and G = shear modulus = $E_c/2(1+\mu)$. Poisson's ratio, μ for normal strength concrete is approximated as 0.30. Then, for normal strength concrete, $G = 1820 \sqrt{f_c'}$ in MPa units. Consistent with Eq. (1), MCFT analyses of columns in the test matrix showed that the uncracked shear stiffness is independent of other parameters such as column aspect ratio, amount of transverse and longitudinal reinforcement. As an example, Fig. 8 shows that the uncracked shear stiffness of Specimen-1 remains unchanged prior to shear cracking if the longitudinal reinforcement ratio is varied.
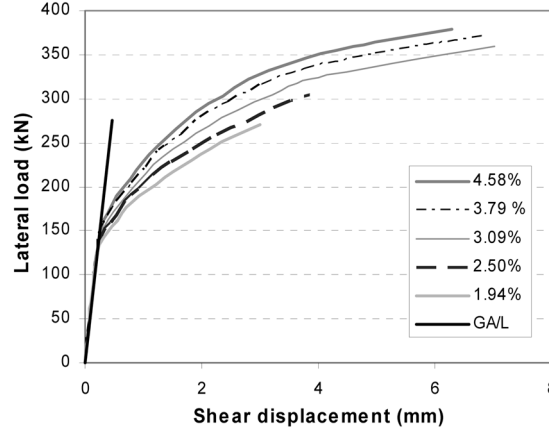
Fig. 8 Effect of longitudinal reinforcement ratio on shear displacement

3.2 Cracking shear strength

Consistent with the trend shown in Fig. 7, the cracking shear strength, V_{cr} (Point A in Fig. 6) is primarily a function of uncracked shear stiffness, GA/L and axial load, P. For columns in the test matrix, V_{cr} values calculated from MCFT analyses are plotted as a ratio of GA/L and as a function of axial load ratio in Fig. 9. Based on regression analysis of results, Eq. (2) is recommended

$$V_{cr} = \left(\frac{P}{2f_c' A_g} + 0.10 \right) \frac{GA}{L} = \left(\frac{P}{2f_c' A_g} + 0.10 \right) \frac{1820 \sqrt{f_c'} A}{L} \qquad (2)$$

In Eq. (2), $P/f_c' A_g$ is unitless, and GA/L has MPa units.

3.3 Maximum shear strength and corresponding average shear strain

There are a number of available existing models to predict the maximum shear strength, V_n of a RC column (at Points B and C in Fig. 6). In this study, Eq. (3) proposed by Sezen and Moehle (2004) is adapted.
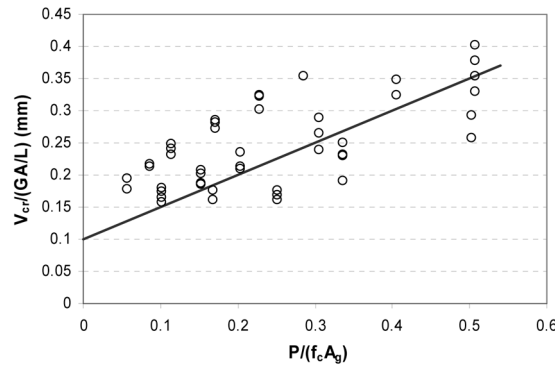

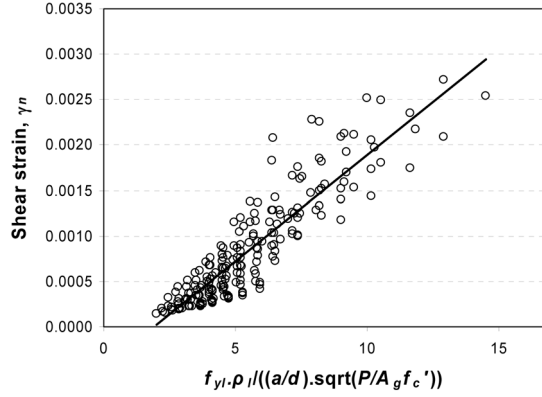Fig. 9 Calculated cracking displacement versus axial load ratio

Fig. 10 Regression analysis of parameters affecting the shear strain at maximum strength

$$V_n \; = \; V_s + V_c \; = \; k\frac{A_v f_{yv} d}{s} + k\left(\frac{0.5\sqrt{f_c'}}{a\,/\,d}\sqrt{1 + \frac{P}{0.5\sqrt{f_c'}\,A_g}}\right)0.8 A_g \; (\mathrm{MPa}) \tag{3}$$

where A_v is cross-sectional area of transverse reinforcement oriented parallel to the applied shear and having longitudinal spacing s. The factor k is defined to be equal to 1.0 for displacement ductility less than 2, to be equal to 0.7 for displacement ductility exceeding 6, and to vary linearly for intermediate displacement ductilities. For columns failing in shear, ideally the maximum shear strength calculated from Eq. (3) and MCFT analysis should be the same.

The average shear strains or shear displacement at the maximum shear strength appear to be influenced by many factors. The effect of each parameter on the calculated average shear strain is investigated by keeping all other parameters constant. For example, it was found that the shear strain is inversely proportional with the square root of axial load ratio, $P/A_g f_c'$ (Patwardhan and Sezen 2006). It was also found that the shear strain varies linearly with the product of longitudinal steel yield strength, f_{yl} and longitudinal steel ratio, ρ_l. Based on regression analyses presented in Fig. 10, a linear relationship is proposed to calculate the shear strain, γ_n at the maximum strength. The unit of f_{yl} is MPa, ρ_l is expressed in percentage, and aspect ratio, a/d and axial load ratio are unitless. The corresponding shear displacement, Δ_n can simply be calculated by multiplying γ_n by the column length, L.

Eq. (4) is valid for columns exhibiting shear-flexure and flexure failures only. In other words, the maximum shear strength V_n is equal to or larger than the shear capacity V_p corresponding to the maximum flexural strength, or plastic hinge moment, M_p, possibly obtained from sectional moment-curvature analysis. V_p can be calculated by dividing M_p by the shear span, a ($=L$ for a cantilever column). The behavior of columns failing in shear before flexural yielding is not investigated here, but reported in Patwardhan (2006).

$$\gamma_n \; = \; \frac{f_{yl} \cdot \rho_l}{5000 \cdot a\,/\,d \cdot \sqrt{\dfrac{P}{A_g f_c'}}} - 0.0004 \tag{4}$$

3.4 Onset of shear strength degradation

The shear response of a column can be predicted reasonably well by the MCFT until the maximum strength is reached (Fig. 4). However, the column experiences additional shear deformations under the sustained lateral load while exhibiting significant strength degradation and an eventual axial load failure. Thus, at least two more points on the shear envelope representing the onset of shear degradation and axial load failure (Points C and D in Fig. 6) need to be defined.

As illustrated in Fig. 5(b), Gerin and Adebar (2004) identifies a point where the shear strength degradation begins in their model. However, their model is based on a theoretical shear displacement at yield and shear strain ductility. The flexural yielding was not considered to be critical in the proposed model. The model by Gerin and Adebar is modified to obtain the ultimate shear strain, γ_u

$$\gamma_n = \left(4 - 12 \frac{v_n}{f_c'} \right) \gamma_n \tag{5}$$

where v_n ($= V_n/bd$, b = width of cross section) is the shear stress at the peak strength (Point B or C in Fig. 6), and the shear strain at the peak strength, γ_n is calculated from Eq. (4). The corresponding shear displacement, Δ_u (at Point C in Fig. 6) can then be obtained by multiplying the shear strain γ_u by the column height.

3.5 Shear displacement at axial load failure

It has been a common practice to stop the column testing in the laboratory as soon as some strength degradation was observed. In recent years, few researchers loaded their test columns beyond the peak strength and after the shear failure until the axial-load-carrying capacity was completely lost. As a result, there is very limited test data including complete response all the way up to axial load failure (Point D in Fig. 6). Consequently, due to lack of experimental evidence, deformation capacities after shear failure were not investigated until recent years. Using a shear friction model and test data, Elwood and Moehle (2005) and Elwood (2004) proposed an equation to calculate the drift ratio at axial load failure for shear-damaged columns.

$$\frac{\Delta_{ALF}}{L} = \frac{4}{100} \frac{1 + \tan^2\theta}{\tan\theta + P\left(\dfrac{s}{A_v f_{yv} d_c \tan\theta} \right)} \tag{6}$$

where θ is the angle of the shear crack and d_c is the depth of the core concrete, measured to the centerlines of the transverse reinforcement. In the derivation, θ was assumed to be 65 degrees. Following the procedure presented in Setzler (2005), the shear displacement at axial load failure (Δ_{af} in Fig. 6) can be calculated by subtracting the maximum flexural and slip displacements from the total lateral displacement, Δ_{ALF}.

4. Model verification

During the vast majority of column experiments, only the total lateral displacement, but not shear

displacements, was measured and reported because it is difficult to measure shear deformations independent of flexural deformations. Accurate measurement of shear deformations requires placing a series of horizontal, vertical and diagonal displacement potentiometers over the height of the specimen. As a result, RC column experimental data with reported shear displacements are scarce. Few column tests with available shear displacement data are used to evaluate the proposed model. The proposed model was applied to six test columns: four columns tested by Sezen and Moehle (2006) and two by Saatcioglu and Ozcebe (1989). Properties of columns and calculated and measured lateral strengths are shown in Tables 1 and 2. The shear cracking and peak strengths, V_{cr} and V_n are calculated from Eqs. (2) and (3), respectively. V_p is the lateral force required to develop maximum flexural moment capacity, M_p which is calculated from moment-curvature analysis of the cross section. $V_{max,MCFT}$ is the maximum lateral strength calculated from Response-2000. The data in Table 2 indicates that the measured maximum lateral strengths, V_{test} compare reasonably well with the strengths predicted from Eqs. (2) and (3) and MCFT analysis. Ideally, $V_{max,MCFT}$ should be equal to the smaller of V_p and V_n. Fig. 11 compares the experimental lateral load-shear displacement

Table 1 Properties of test columns

Column	a	b	a/d	f_c'	f_{yl}	f_{yv}	ρ_l	ρ_v	s	P	$P/A_g f_c'$	μ_δ
	mm	mm		MPa	MPa	MPa	%	%	mm	kN		
Saatcioglu and Ozcebe (1989)												
U1	1000	350	3.28	43.6	430	470	3.8	0.27	150	0	0	3.12
U6	1000	350	3.28	37.3	437	425	3.8	0.84	65	600	0.13	7.37
Sezen and Moehle (2006)												
Specimen-1	1473	457	3.76	21.1	447	469	2.5	0.17	305	667	0.15	2.88
Specimen-2	1473	457	3.76	21.1	447	469	2.5	0.17	305	2669	0.61	1.29
Specimen-3	1473	457	3.76	20.9	447	469	2.5	0.17	305	var.[*]	var.[*]	2.72
Specimen-4	1473	457	3.76	25.6	447	469	2.5	0.17	305	667	0.15	3.14

*Specimen-3 was tested under varying axial load.

Table 2 Test column strengths

Column	V_{cr}	V_n	V_p	$V_{max,MCFT}$	V_{test}
	kN	kN	kN	kN	kN
Saatcioglu and Ozcebe (1989)					
U1	147	228	290	246	276
U6	225	368	362	360	343
Sezen and Moehle (2006)					
Specimen-1	104	285	303	315	315
Specimen-2	240	409	308	328	359
Specimen-3-H[*]	209	409	308	338	301
Specimen-3-L[*]	88	234	258	238	247
Specimen-4	114	281	305	315	294

*High and low axial loads for Specimen-3 are 2669 kN (H[*]) and 249 kN (L[*]), respectively.
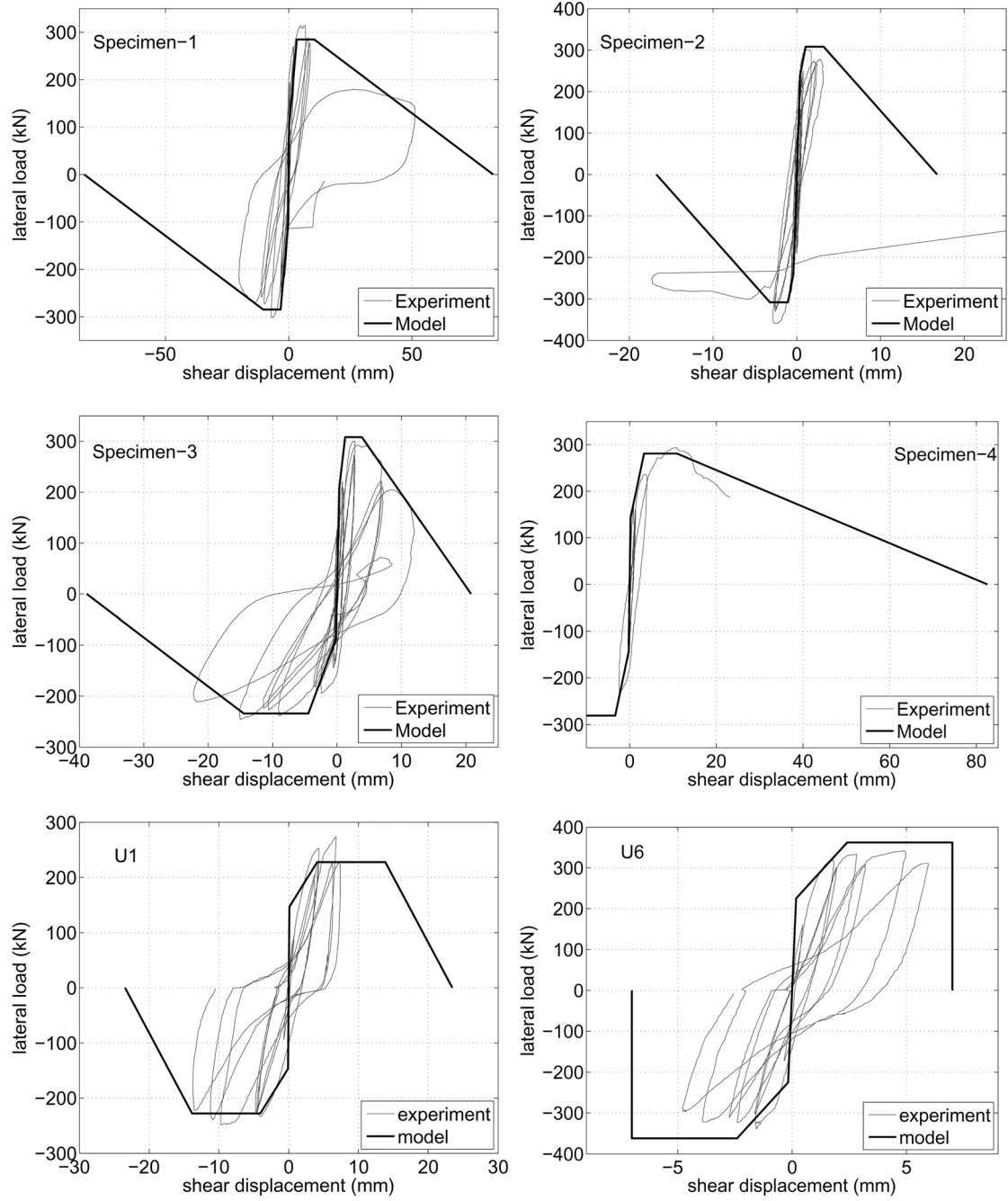
Fig. 11 Lateral load-shear displacement relations for columns tested by Sezen and Moehle (2006) and Saatcioglu and Ozcebe (1989)

relations with the monotonic response envelope predicted using the proposed model. Overall, the measured and calculated responses show a good agreement.

5. Conclusions

A model was proposed to predict the monotonic shear response of reinforced concrete columns. The model predicts the shear displacements and strengths at certain critical response stages, including first shear cracking, peak strength, onset of shear failure, and axial load failure. The shear displacements at first shear cracking and at the maximum strength are predicted from simplified equations which were defined using the results from the Modified Compression Field Theory, MCFT analyses of a large number of columns. In order to predict the shear response at the onset of shear degradation, a slightly modified version of an existing model was used. Due to lack of test data as well as models for predicting displacements at axial load failure, a widely used existing model for total lateral displacement was adapted. Then, the shear displacement is calculated as the difference between the total lateral displacement and the maximum flexural and slip displacements. The predictions from the proposed model are in good agreement with the scarcely available experimental data.

References

AASHTO (2000), American Association of State Highway Transportation Officials, "LRFD Bridge Design Specifications and Commentary".

ACI 318-05 (2005), Building Code Requirements for Structural Concrete and Commentary. American Concrete Institute, Farmington Hills, Mich.

ASCE-ACI Task Committee 426 (1973), "The shear strength of reinforced concrete members", *J. Struct. Div.*, ASCE, **99**(6), 1091-1187.

Aschheim, M., Gulkan, P., Sezen, H., Bruneau, M., Elnashai, A., Halling, M., Love, J. and Rahnama, M. (2000), "Performance of buildings", *Kocaeli, Turkey Earthquake of August 17, 1999 Reconnaissance Report. Earthq. Spectra*, Supplement A, **16**, 237-279.

Bentz, E. (2000), "Sectional analysis of reinforced concrete members", *Ph.D. Dissertation,* University of Toronto. 310.

Dogangun, A. (2004), "Performance of reinforced concrete buildings during the May 1, 2003 bingol earthquake in turkey", *Eng. Struct.*, **26**, 841-856.

Elwood, K.J. (2004), "Modeling failures in existing reinforced concrete columns", *Can. J. Civil Eng.*, **31**, 846-859.

Elwood, K.J. and Moehle, J.P. (2005), "Axial capacity model for shear-damaged columns", *ACI Struct. J.,* **102**(4), 578-587.

Gerin, M. and Adebar, P. (2004), "Accounting for shear in seismic analysis of concrete structures", *Proc. of the 13th World Conf. on Earthquake Engineering,* Vancouver, August. Paper No. 1747.

Hsu, T.T.C. (1988), "Softened truss model for shear and torsion", *ACI Struct. J.*, **85**(6), 624-635.

Hsu, T.T.C. and Zhu, R.R.H. (2002), "Softened membrane model for reinforced concrete elements in shear", *ACI Struct. J.*, **99**(4), 460-469.

Lee, D.H. and Elnashai, A.S. (2001), "Seismic analysis of RC bridge columns with flexure-shear interaction", *J. Struct. Eng.,* ASCE, **127**(5), 546-553.

Lehman, D.E. and Moehle, J.P. (2000), "Seismic performance of well-confined concrete bridge columns", *Pacific Earthquake Engineering Research Center, University of California, Berkeley*, Report No. PEER-98/01, 316.

Maruyama, M. and Jirsa, J.O. (1979), "Shear behavior of reinforced concrete members under bidirectional reversed lateral loading", *CESRL Report No.78-1, University of Texas, Austin*.

Mostafaei, H. and Kabeyasawa, T. (2007), "Axial-shear-flexure interaction approach for reinforced concrete columns", *ACI Struct. J.,* **104**(2), 218-226.

Ozcebe, G. and Saatcioglu, M. (1989), "Hysteretic shear model for reinforced concrete members", *J. Struct. Eng.,*

115(1), 132-148.

Panagiotakos, T.B. and Fardis, M.N. (2001), "Deformations of reinforced concrete members at yielding and ultimate", *ACI Struct. J.*, **98**(2), 135-148.

Park, R. and Paulay, T. (1975), *Reinforced Concrete Structures*, John Wiley & Sons Inc., New York.

Patwardhan, C.V. (2005), "Shear strength and deformation modeling of reinforced concrete columns", *M.S. Thesis.* The Ohio State University. 176.

Pincheira, J.A., Dotiwala, F.S. and D'Souza, J.T. (1999), "Seismic analysis of older reinforced concrete columns", *Earthq. Spectra*, **15**(2), 245-272.

Priestley, M.J.N., Verma, R. and Xiao, Y. (1994), "Seismic shear strength of reinforced concrete columns", *J. Struct. Eng.*, ASCE, **120**(8), 2310-2329.

Priestley, M.J.N., Ranzo, G., Benzoni, G. and Kowalsky, M. (1996), "Yield displacement of circular bridge columns", *Fourth CalTrans Research Workshop*, Sacramento, California, July.

Saatcioglu, M. and Ozcebe, G. (1989), "Response of reinforced concrete columns to simulated seismic loading", *ACI Struct. J.*, **86**(3), 3-12.

Sezen, H. (2002), "Seismic behavior and modeling of reinforced concrete building columns", *Ph.D. Dissertation,* University of California, Berkeley. 345.

Sezen, H. and Moehle, J.P. (2006), "Seismic tests of concrete columns with light transverse reinforcement", *ACI Struct. J.*, **103**(6), 842-849.

Sezen, H. and Moehle, J.P. (2004), "Shear strength model for lightly reinforced columns", *J. Struct. Eng.*, ASCE. **130**(11), 1692-1703.

Sezen, H. and Patwardhan, C.V. (2006), "Shear displacement model for reinforced concrete columns", *Proc. of the ASCE Structures Conf.*, St Louis, Missouri, May.

Setzler, E.J. (2005), "Modeling the behavior of lightly reinforced concrete columns subjected to lateral loads", *M.S. Thesis*. The Ohio State University, 202.

Setzler, E.J. and Sezen, H. (2007), "Model for lateral behavior of reinforced concrete columns including shear deformations", *Earthq. Spectra*. (Accepted for publication)

Takayanagi, T., Derecho, A.T. and Corley, W.G. (1979), "Analysis of inelastic shear deformation effects in R/C structural wall systems", *Proc., Nonlinear Design of Conc. Struct., CSCE-ASCE-ACI-CEB Int. Symp.*, Univ. of Waterloo Press, Waterloo, Canada, 545-579.

Vecchio, F.J. and Collins, M.P. (1986), "The modified compression-field theory for reinforced concrete elements subjected to shear", *ACI Struct. J.*, **83**(2), 219-231.

Vecchio, F.J. and Collins, M.P. (1988), "Predicting the response of reinforced concrete beams subjected to shear using the modified compression field theory", *ACI Struct. J.*, **85**(3), 258-268.